Eur. Phys. J. C 44, 175–182 (2005)
Digital Object Identifier (DOI) 10.1140/epjc/s2005-02371-1

THE EUROPEAN PHYSICAL JOURNAL C

Determining the stau trilinear coupling A_τ in supersymmetric Higgs decays

S.Y. Choi[1], H.-U. Martyn[2,a], P.M. Zerwas[3]

[1] Department of Physics, Chonbuk National University, Chonju, Korea
[2] I. Physikalisches Institut, RWTH Aachen, Germany
[3] Deutsches Elektronensynchrotron DESY, Hamburg, Germany

Received: 2 August 2005 /
Published online: 13 September 2005 –

Abstract. The measurement of the trilinear couplings A in the part of the Lagrangian which breaks supersymmetry softly will be a difficult experimental task. In this report the heavy Higgs decays $H, A \to \tilde{\tau}_1\tilde{\tau}_2$ to stau pairs are investigated for measuring the stau trilinear coupling A_τ. Based on detailed simulations of signal and backgrounds for a specific reference point in future high luminosity e^+e^- linear collider experiments, it is concluded that the parameter A_τ can be determined with a precision at the 10% level in the region of moderate to large $\tan\beta$.

1 Introduction

The couplings between fermionic matter fields and Higgs fields differ from those of the scalar matter fields once supersymmetry is broken, see e.g. [1]. In theories based on soft supersymmetry breaking the scalar-Higgs Yukawa couplings are modified multiplicatively by the A parameters which, in parallel to the fermion-Higgs Yukawa couplings, are inter-generational matrices. In accordance with bounds on flavor-changing couplings the A parameters are generally assumed to be diagonal and three parameters, A_t, A_b and A_τ, are introduced for the third generation.

By definition, the A parameters come with the Yukawa couplings which are of the size of the fermion masses. Therefore they cannot be measured in general directly except for the third generation. Since they couple Higgs fields with scalar L-fields and R-fields, they become effective in two ways: (i) They contribute to the off-diagonal elements in the scalar mass matrices, and to the mixing of L- and R-states; and (ii) They give rise to mixed scalar L and R decay final states of the heavy scalar and pseudoscalar Higgs bosons.

In the scalar stop sector the off-diagonal mass matrix element is given by $m_t(A_t - \mu\cot\beta)$. For moderate to large $\tan\beta$ the second term is suppressed and A_t can be determined quite accurately by measuring the mixing effects in the stop mass spectrum and the stop mixing angle in e^+e^- annihilation to stop pairs [2]. In heavy Higgs decays, on the other hand, A_t is shielded by the potentially much larger term $\mu\tan\beta$ and Higgs decays to stop pairs, if kinematically allowed at all, are less suited for measuring the stop trilinear parameter.

[a] e-mail: martyn@desy.de

The situation is reversed in the down sector, i.e. for staus. While in the stau system A_τ is shielded by the term $\mu\tan\beta$ in the mass matrix [3], the A_τ parameter is enhanced by the coefficient $\tan\beta$ in the couplings of the heavy scalar and pseudoscalar Higgs bosons to mixed pairs of $\tilde{\tau}_L$ and $\tilde{\tau}_R$ fields. Heavy Higgs decays are therefore promising channels for measuring the stau trilinear parameter A_τ.

The expressions for the partial decay widths become especially transparent in the limit where (i) the heavy Higgs boson masses are large [decoupling limit], (ii) $\tan\beta$ is large, and (iii) the LR mixing is small. In this limit the decay widths of the scalar and pseudoscalar Higgs bosons to mixed pairs $\tilde{\tau}_1\tilde{\tau}_2 \equiv \tilde{\tau}_1^+\tilde{\tau}_2^- + \tilde{\tau}_1^-\tilde{\tau}_2^+$ are given by

$$\Gamma(H, A \to \tilde{\tau}_1\tilde{\tau}_2) \simeq \frac{G_F m_\tau^2}{4\sqrt{2}\pi}\,\lambda^{1/2}\,\frac{(A_\tau\tan\beta+\mu)^2}{m_{H,A}}\,, \quad (1)$$

where λ accounts for the phase space suppression in the usual form. The couplings of the scalar Higgs boson H to diagonal pairs of L- and R-fields are suppressed by coefficients m_τ/A_τ and $m_Z/(A_\tau\tan\beta)$ which both are small in the limit we are considering. The coupling of the pseudoscalar Higgs boson A to diagonal pairs vanishes in CP-invariant theories.

Using the partial widths for Higgs decays to tau pairs,

$$\Gamma(H, A \to \tau\tau) \simeq \frac{G_F m_\tau^2}{4\sqrt{2}\pi}\,m_{H,A}\,\tan^2\beta\,, \quad (2)$$

the decay widths to stau pairs may be normalized by the decays to tau pairs:

$$\frac{\Gamma(H, A \to \tilde{\tau}_1\tilde{\tau}_2)}{\Gamma(H, A \to \tau\tau)} \simeq \lambda^{1/2}\,\frac{(A_\tau+\mu\,\cot\beta)^2}{m_{H,A}^2}\,. \quad (3)$$

If the normalization is chosen alternatively by the dominating $b\bar{b}$ final states, the ratio of the widths is reduced by a coefficient $m_\tau^2/3m_b^2$:

$$\frac{\Gamma(H, A \to \tilde{\tau}_1\tilde{\tau}_2)}{\Gamma(H, A \to b\bar{b})} \simeq \lambda^{1/2}\, \frac{m_\tau^2}{3m_b^2}\, \frac{(A_\tau + \mu\, \cot\beta)^2}{m_{H,A}^2}\,. \quad (4)$$

In any case, for moderate to large $\tan\beta$ and A_τ of the same order as μ, the size of the branching ratio of the heavy Higgs bosons to mixed LR stau pairs is essentially set by A_τ^2. Thus, for sufficiently large A_τ the measurement of these branching ratios provides a valuable instrument for measuring A_τ.

2 Properties of the Higgs system

The qualitative arguments presented above appear strong enough to perform a quantitative analysis in order to prove this method to be useful for measuring A_τ in practice. For this purpose we adopt the mSUGRA reference point SPS1a′ defined for the *SPA Project* [4]. It is closely related to the standard reference point SPS1a, yet with a cold dark matter density in accordance with the WMAP measurement.

The mSUGRA parameters are defined as $M_0 = 70\,\text{GeV}$, $M_{1/2} = 250\,\text{GeV}$, $A_0 = -300\,\text{GeV}$, $\tan\beta = 10$ and sign $\mu = +$. Extrapolation to the electroweak scale generates the Lagrangian parameters $A_\tau = -445\,\text{GeV}$ and $\mu = 403\,\text{GeV}$, thus $|A_\tau| \gg \mu\cot\beta$ holds indeed. The masses and branching ratios of the supersymmetric particles relevant to the present analysis are summarized in Table 1.

At a linear collider with an energy $\sqrt{s}$ of about 1 TeV heavy Higgs boson production $e^+e^- \to HA$, see [6], will clearly be kinematically accessible for this reference point [7]. The measurement of their decay modes, however, will confront several problems:

- Due to their mass degeneracy the decays of H and A cannot be resolved experimentally. Thus one can only determine the branching ratios for the sum of both Higgs bosons.
- The energy spectra of the final τ decay products reflect only weakly the energy of the primary particles, which is gradually softened during cascade decays involving massive invisible particles like neutralinos or sneutrinos. It is therefore extremely difficult to discriminate $\tilde{\tau}_1$ from $\tilde{\tau}_2$ decays. Instead, only the sum of all $\tilde{\tau}_i\tilde{\tau}_j$ decay modes will be determined.
- As a consequence of the (moderately) large value $\tan\beta = 10$ the neutralino $\tilde{\chi}_2^0$ and chargino $\tilde{\chi}_1^\pm$ decays lead preferentially to final states involving τ leptons. Abundant multi-tau signatures constitute a severe background to all channels involving SUSY particles, in particular to the decays of interest $H, A \to \tilde{\tau}_i\tilde{\tau}_j$.

The strategy to determine the H, A decay modes and branching ratios is the tagging of one Higgs particle by its decay into a pair of $b\bar{b}$ jets and the analysis of the recoiling system:

$$e^+e^- \to HA \to b\bar{b}\,X\,. \quad (5)$$

Table 1. Masses and branching ratios of heavy Higgs bosons, light gauginos and third generation sleptons in the SPS1a′ scenario [4]. The Higgs decays are calculated with the program FeynHiggs 2.2.10 [5]

Particle	Mass [GeV]	Decay	$\mathcal{B}$	Decay	$\mathcal{B}$
H^0	431.1	$\tau^-\tau^+$	0.075	$\tilde{\chi}_1^0\tilde{\chi}_1^0$	0.011
		$b\bar{b}$	0.683	$\tilde{\chi}_1^0\tilde{\chi}_2^0$	0.040
		$t\bar{t}$	0.053	$\tilde{\chi}_2^0\tilde{\chi}_2^0$	0.023
		$\tilde{\tau}_1^-\tilde{\tau}_1^+$	0.014	$\tilde{\chi}_1^+\tilde{\chi}_1^-$	0.056
		$\tilde{\tau}_1^\mp\tilde{\tau}_2^\pm$	0.031		
		$\tilde{\tau}_2^-\tilde{\tau}_2^+$	0.003		
A^0	431.0	$\tau^-\tau^+$	0.055	$\tilde{\chi}_1^0\tilde{\chi}_1^0$	0.011
		$b\bar{b}$	0.505	$\tilde{\chi}_1^0\tilde{\chi}_2^0$	0.055
		$t\bar{t}$	0.103	$\tilde{\chi}_2^0\tilde{\chi}_2^0$	0.063
		$\tilde{\tau}_1^\mp\tilde{\tau}_2^\pm$	0.035	$\tilde{\chi}_1^+\tilde{\chi}_1^-$	0.170
$\tilde{\chi}_1^0$	97.8				
$\tilde{\chi}_2^0$	184.4	$\tilde{\tau}_1^\pm\tau^\mp$	0.564	$\tilde{\nu}_\tau\nu_\tau$	0.155
		$\tilde{e}_R^\pm e^\mp$	0.024	$\tilde{\nu}_e\nu_e$	0.115
		$\tilde{\mu}_R^\pm\mu^\mp$	0.026	$\tilde{\nu}_\mu\nu_\mu$	0.115
$\tilde{\chi}_1^+$	184.2	$\tilde{\tau}_1^+\nu_\tau$	0.519	$\tilde{\nu}_\tau\tau^+$	0.189
				$\tilde{\nu}_e e^+$	0.138
				$\tilde{\nu}_\mu\mu^+$	0.138
$\tilde{\tau}_1$	107.4	$\tilde{\chi}_1^0\tau^-$	1.000		
$\tilde{\tau}_2$	195.3	$\tilde{\chi}_1^0\tau^-$	0.869	$\tilde{\chi}_1^-\nu_\tau$	0.086
		$\tilde{\chi}_2^0\tau^-$	0.046		
$\tilde{\nu}_\tau$	170.7	$\tilde{\chi}_1^0\nu_\tau$	1.000		

The decay modes and event topologies under investigation are

$$X_{\tilde{\tau}_i\tilde{\tau}_j} = \tilde{\tau}_1\tilde{\tau}_1 + \tilde{\tau}_1\tilde{\tau}_2 + \tilde{\tau}_2\tilde{\tau}_2 \to \tau^+\tau^-\not{E}, \quad (6)$$

$$X_{\tilde{\chi}_i^0\tilde{\chi}_2^0} = \tilde{\chi}_1^0\tilde{\chi}_2^0 + \tilde{\chi}_2^0\tilde{\chi}_2^0 \to \tau^+\tau^-\not{E}, \quad (7)$$

$$X_{\tilde{\chi}_1^+\tilde{\chi}_1^-} = \tilde{\chi}_1^+\tilde{\chi}_1^- \to \tau^+\tau^-\not{E}, \quad (8)$$

and the reference decay modes are

$$X_{\tau\tau} = \tau^+\tau^-\,, \quad (9)$$

$$X_{b\bar{b}} = b\bar{b} \to jet\,jet\,. \quad (10)$$

The particle content of the three supersymmetric final states (6)–(8) is identical. In order to distinguish these channels it will be assumed that the masses of the primary and of all the secondary SUSY particles are known well enough so that the resulting decay topologies and $\tau^\pm$ spectra can be reliably modeled and simulated. This knowledge is important in order to determine the branching ratios of the various decay modes from their relative contributions to the 'observable' data distributions. This assumption is quite natural as the measurement of the A parameters is certainly a second-generation task. Details of the event generation are presented in the Appendix A.

The cross sections for HA pair production [6] assuming common scalar and pseudoscalar Higgs masses are shown

Table 2. Event selection criteria for the signal reaction $HA \to b\bar{b}\,\tilde{\tau}_i\tilde{\tau}_j \to b\bar{b}\,\tau^+\tau^-\not{E}$

Selection criteria		Constraint
1	two identified b jets	
2	b jet energy	$100\,\text{GeV} < E_b < 400\,\text{GeV}$
3	bb invariant mass	$m_{H,A} - 30\,\text{GeV} < m_{bb} < m_{H,A} + 30\,\text{GeV}$
	recoil mass against bb	$m_{H,A} - 30\,\text{GeV} < m_{\text{recoil}} < m_{H,A} + 90\,\text{GeV}$
4	two oppositely charged τ candidates	
5	visible τ energy	$2.5\,\text{GeV} < E_\tau < 200\,\text{GeV}$
	visible $\tau\tau$ energy	$E_{\tau\tau} < 250\,\text{GeV}$
6	missing energy	$250\,\text{GeV} < \not{E} < 550\,\text{GeV}$
7	acollinearity angle in Higgs rest frame	$\xi^*_{\tau\tau} > 10^\circ$

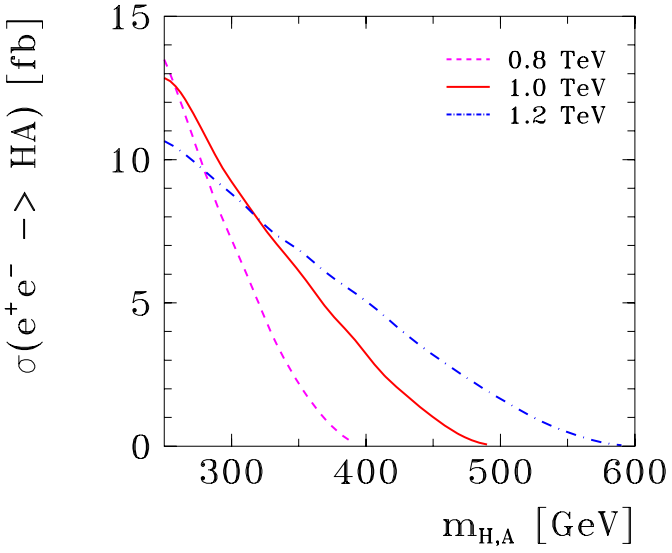

Fig. 1. Cross section for $e^+e^- \to HA$ production as a function of the common H, A mass at $\sqrt{s} = 0.8$ TeV, 1.0 TeV and 1.2 TeV. The curves include $e^\pm$ beam polarizations of $\mathcal{P}_{e^-} = \pm 0.9$ and $\mathcal{P}_{e^+} = \mp 0.6$, as well as QED radiation and beamstrahlung effects

in Fig. 1 for the three center of mass energies $\sqrt{s} = 0.8$ TeV, 1.0 TeV and 1.2 TeV. The remaining parameters are taken from the reference point SPS1a′ for illustration. The present study is representative and based on 10,000 HA events which, for scenario SPS1a′, may be accumulated with a cross section of 1.8 fb at 1 TeV or 3.9 fb at 1.2 TeV, respectively. The results may be easily scaled to lower statistics event samples without losing their significance.

3 Experimental analysis

In this section the analyses of reaction (5) with the Higgs decay modes (6)–(10) will be described in detail. As mentioned above the channels involving supersymmetric particles, $X_{\tilde{\tau}_i\tilde{\tau}_j}$, $X_{\tilde{\chi}^0_i\tilde{\chi}^0_2}$ and $X_{\tilde{\chi}^+_1\tilde{\chi}^-_1}$, lead to the same final state and the topologies do not allow their separation on an event-by-event basis. Rather a statistical analysis will be applied to determine their branching fractions. The decays into Standard Model particles, $X_{\tau\tau}$ and $X_{b\bar{b}}$, can be efficiently isolated and will be used for normalization. The results will be given in terms of combined branching ratios, defined as $\mathcal{B}_{b\bar{b}\,X} = \mathcal{B}(H \to b\bar{b})\,\mathcal{B}(A \to\ X) + \mathcal{B}(A \to b\bar{b})\,\mathcal{B}(H \to\ X)$.

It should be noted that the results for the background Higgs decays to charginos and neutralinos can probably be predicted at the time of the stau analyses. They depend only on parameters which can be measured in the chargino/neutralino sector itself at earlier times. This way the experimental results of the Higgs decays to charginos and neutralinos can be compared with theoretical predictions.

3.1 Signal channel $e^+e^- \to HA \to b\bar{b}\,\tau^+\tau^-\not{E}$

The topology is characteristic for all Higgs decays into supersymmetric particles. The criteria listed in Table 2 are chosen in order to optimize the acceptance for $HA \to b\bar{b}\,\tilde{\tau}_i\tilde{\tau}_j \to b\bar{b}\,\tau^+\tau^-\not{E}$ decays.

The criteria (1)–(3) provide a very efficient selection of $HA \to b\bar{b}X$ events by tagging one Higgs particle via its resonant decay into a pair of b quark jets [see discussion in Appendix A and Fig. 6]. The good energy resolution allows the reliable transformation into the rest frame of the recoil system X which is identified as the second Higgs particle.

The criteria (4)–(6) select SUSY decays into secondary $\tau's$ plus large missing energy. The last cut (7) removes direct decays into $\tau\tau$ pairs, which are back-to-back in the Higgs rest frame. The properties of the various decay modes are displayed in the left panels of Fig. 2, where normalized distributions of the visible tau energy and di-tau mass are shown. It is a common feature of both spectra that the dominant contributions come from $\tilde{\chi}^+_1\tilde{\chi}^-_1$ peaks at low values, while the spectra from $\tilde{\tau}_i\tilde{\tau}_j$ and $\tilde{\chi}^0_i\tilde{\chi}^0_2$ extend towards higher values. The separation between the decay modes improves when correlations between both particles are exploited, e.g. the invariant mass $m_{\tau\tau}$. Also notice that the shapes of the distributions from $\tilde{\chi}^0_1\tilde{\chi}^0_2$ and $\tilde{\chi}^0_2\tilde{\chi}^0_2$ are barely distinguishable, thus only the sum of all neutralino decays, labeled $\tilde{\chi}^0_i\tilde{\chi}^0_2$, will be investigated.

The overall $H, A \to \tilde{\tau}_i\tilde{\tau}_j$ efficiency is $\sim 43\%$. However, there are still large contributions from Higgs decays into

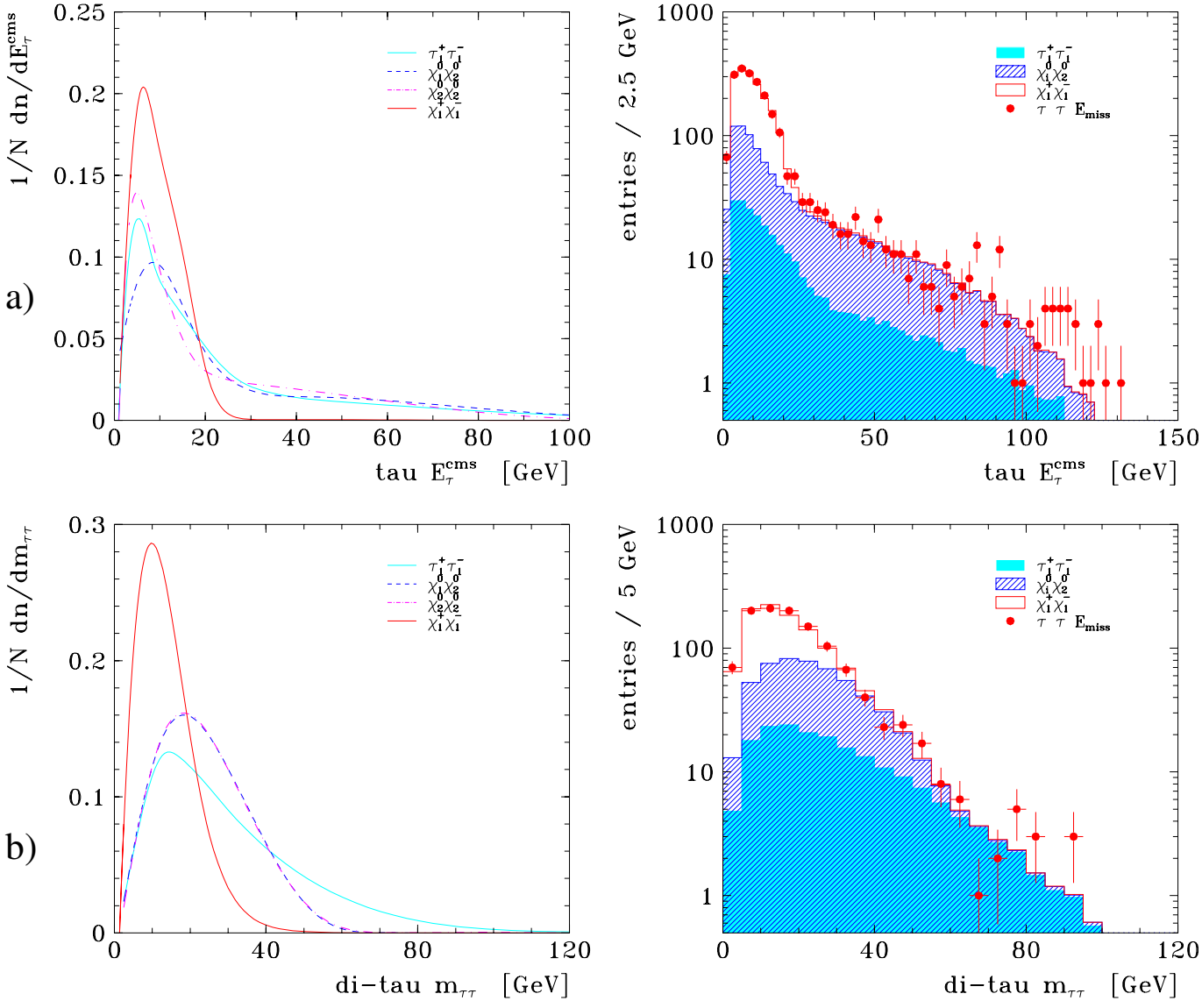

Fig. 2. Spectra from $e^+e^- \to HA \to b\bar{b}\,\tau^+\tau^-\not{E}$ decays of **a** visible tau energy E_τ^* in the H, A rest frame; **b** di-tau mass $m_{\tau\tau}$. Left: normalized distributions; right: fitted contributions of individual channels $\tilde{\tau}_i\tilde{\tau}_j$, $\tilde{\chi}_i^0\tilde{\chi}_2^0$ and $\tilde{\chi}_1^+\tilde{\chi}_1^-$ to the observable signal. mSUGRA scenario SPS1a′ at $\sqrt{s} = 1\,\text{TeV}$

charginos ($\sim 37\%$) and neutralinos ($\sim 23\%$), both of which have higher combined branching ratios, see Table 1.

The distributions from the complete simulation of the visible τ energy in the Higgs rest frame E_τ^* and the di-tau mass $m_{\tau\tau}$ are shown in the right panels of Fig. 2. The contributions from the individual decay modes, $X_{\tilde{\tau}_i\tilde{\tau}_j}$, $X_{\tilde{\chi}_i^0\tilde{\chi}_2^0}$ and $X_{\tilde{\chi}_1^+\tilde{\chi}_1^-}$ of eqs. (6)–(8), are summed up and fitted to reproduce the data of Fig. 2. The analyses of the observables E_τ^* and $m_{\tau\tau}$ emphasize different characteristics but lead to consistent results. In all fits (including observables not shown) the chargino contribution can be determined in a stable manner whereas the stau and neutralino parts are strongly correlated.

The fit results are displayed in the spectra of Fig. 2. The relative rates, acceptances and the extracted combined branching ratios $\mathcal{B}_{b\bar{b}X}$ are summarized in Table 3.

Table 3. Expected accuracies on the determination of Higgs decays $HA \to b\bar{b}X$. Listed are the analyzed event samples, the fitted contributions of decay modes $f_{b\bar{b}X}^{\text{fit}}$, the detection efficiencies $\epsilon_{b\bar{b}X}$, and the combined branching ratios $\mathcal{B}_{b\bar{b}X}$. The results are based on 10,000 HA decays in the SPS 1a′ scenario

$e^+e^- \to HA \to b\bar{b}X$	$f_{b\bar{b}X}^{\text{fit}}$	$\epsilon_{b\bar{b}X}$	$\mathcal{B}_{b\bar{b}X}$
$HA \to b\bar{b}\,\tilde{\tau}_i\tilde{\tau}_j$	0.186 ± 0.041	0.428	0.049 ± 0.011
$b\bar{b}\,\tilde{\chi}_i^0\tilde{\chi}_2^0$	0.292 ± 0.052	0.228	0.135 ± 0.024
$b\bar{b}\,\tilde{\chi}_1^+\tilde{\chi}_1^-$	0.516 ± 0.036	0.372	0.146 ± 0.010
$HA \to b\bar{b}\,\tau\tau$		0.515	0.075 ± 0.004
$HA \to b\bar{b}\,b\bar{b}$		0.630	0.345 ± 0.007

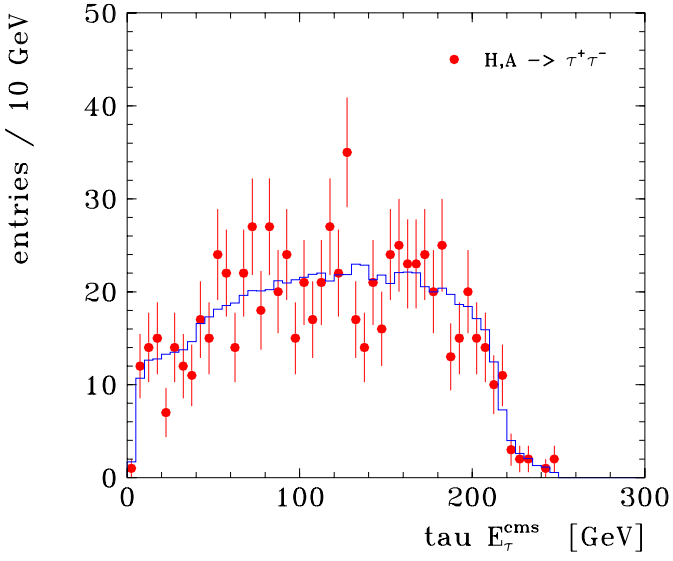

Fig. 3. Spectrum of the visible τ energy E_τ^* in the H, A rest frame from $e^+e^- \to HA \to b\bar{b}\,\tau^+\tau^-$ decays. mSUGRA scenario SPS1a′ at $\sqrt{s} = 1\,\text{TeV}$

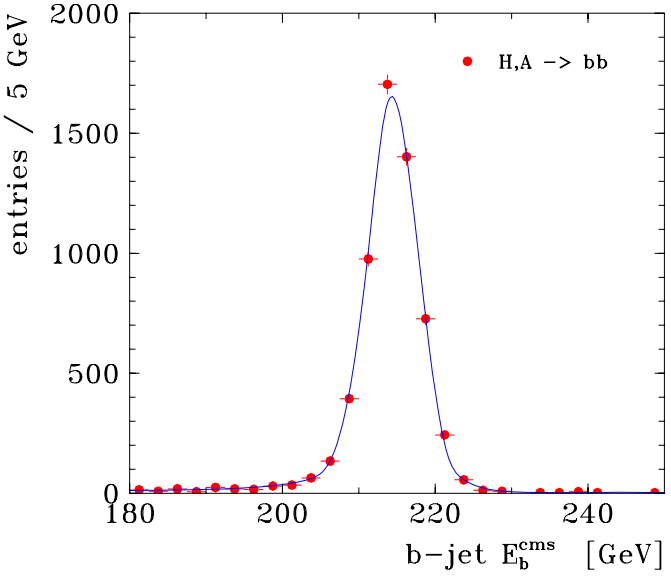

Fig. 4. Spectrum of b-jet energy E_b^* in the H, A rest frame from $e^+e^- \to HA \to b\bar{b}\,b\bar{b}$ decays. mSUGRA scenario SPS1a′ at $\sqrt{s} = 1\,\text{TeV}$

3.2 Reference channels $e^+e^- \to HA \to b\bar{b}\,\tau\tau$ and $HA \to b\bar{b}\,b\bar{b}$

$e^+e^- \to HA \to b\bar{b}\,\tau^+\tau^-$

The selection of $HA \to b\bar{b}\,\tau^+\tau^-$ decays is complementary to the analysis of the previous SUSY decays. The basic criteria (1)–(4) of Table 2 for bb and $\tau\tau$ identification are applied. However, the τ energy spectra are harder and both $\tau's$ are emitted back-to-back in the Higgs rest frame, leading to the following cuts: (5) visible τ energy $5 < E_\tau < 400\,\text{GeV}$, $\tau\tau$ energy $E_{\tau\tau} < 500\,\text{GeV}$; (6) no missing energy requirement; (7) acollinearity angle in the Higgs rest frame $\xi^*_{\tau\tau} < 10°$.

The reconstructed spectrum of the visible τ energy E_τ^* in the Higgs rest frame, shown in Fig. 3, is fairly flat and extends up to the energy of the primary, undecayed τ lepton. The overall detection efficiency is high, see Table 3. A combined branching ratio of $\mathcal{B}_{b\bar{b}\,\tau\tau} = 0.075 \pm 0.004$ can be obtained, where only statistical uncertainties are given. The analysis may be further improved by an overconstrained kinematical fit. Exploiting energy-momentum conservation and approximating the τ directions by the directions of the decay products and treating the τ energies as free parameters, allows one to construct 2 constraints (2-C fit), see [8].

$e^+e^- \to HA \to b\bar{b}\,b\bar{b}$

The selection of $HA \to b\bar{b}\,b\bar{b}$ events is straightforward by applying the same criteria (1)–(3) of Table 2 to another pair of bb jets. The four jets are then combined such as to construct two bb systems with invariant masses closest to each other, $m_{bb}^{(1)} \simeq m_{bb}^{(2)}$. Again, the selection efficiency is high. The energy distribution of the b jets in the Higgs rest frame, displayed in Fig. 4, exhibits a clear signal of a narrow peak at half the Higgs mass. The combined branching ratio for the decay mode $X_{b\bar{b}}$ can be determined with a statistical accuracy of $\mathcal{B}_{b\bar{b}\,b\bar{b}} = 0.345 \pm 0.007$, for details see Table 3.

The measurement only provides information on the product of cross section times branching ratio. In order to extract the decay rates the HA production cross section has to be calculated accurately, which in turn requires a precise knowledge of the Higgs masses. The b jet energy distribution of Fig. 4 (or equivalently the bb mass spectrum similar to Fig. 6a) can be used to determine the H, A masses with an accuracy of $\delta m_{H,A} \simeq 0.15\,\text{GeV}$. This error can be reduced further by applying kinematic fitting techniques [8]. In fact such a procedure allows the selection of a very clean HA event sample with low background, so that relaxing of the b quark identification criteria may be envisaged.

4 Interpretation and conclusions

The expected results for the combined branching ratios of Higgs decay modes (6)–(10) are summarized in Table 3. The double ratios are experimentally determined as $\mathcal{B}_{b\bar{b}\,\tilde{\tau}_i\tilde{\tau}_j}/\mathcal{B}_{b\bar{b}\,b\bar{b}} = 0.142 \pm 0.032$ and $\mathcal{B}_{b\bar{b}\,\tilde{\tau}_i\tilde{\tau}_j}/\mathcal{B}_{b\bar{b}\,\tau\tau} = 0.653 \pm 0.147$. Their relations to the partial decay widths can be written as[1]

$$\frac{\mathcal{B}_{b\bar{b}\,\tilde{\tau}_i\tilde{\tau}_j}}{\mathcal{B}_{b\bar{b}\,b\bar{b}}} = \frac{\mathcal{B}(H \to b\bar{b})\,\mathcal{B}(A \to \tilde{\tau}_1\tilde{\tau}_2) + \mathcal{B}(A \to b\bar{b})\,\mathcal{B}(H \to \tilde{\tau}_i\tilde{\tau}_j)}{\mathcal{B}(H \to b\bar{b})\,\mathcal{B}(A \to b\bar{b})}$$

[1] As mentioned earlier, the pseudoscalar Higgs boson A decays only to off-diagonal $\tilde{\tau}_1\tilde{\tau}_2$ pairs in CP-invariant theories while the scalar Higgs boson H can decay to all combinations of stau pairs

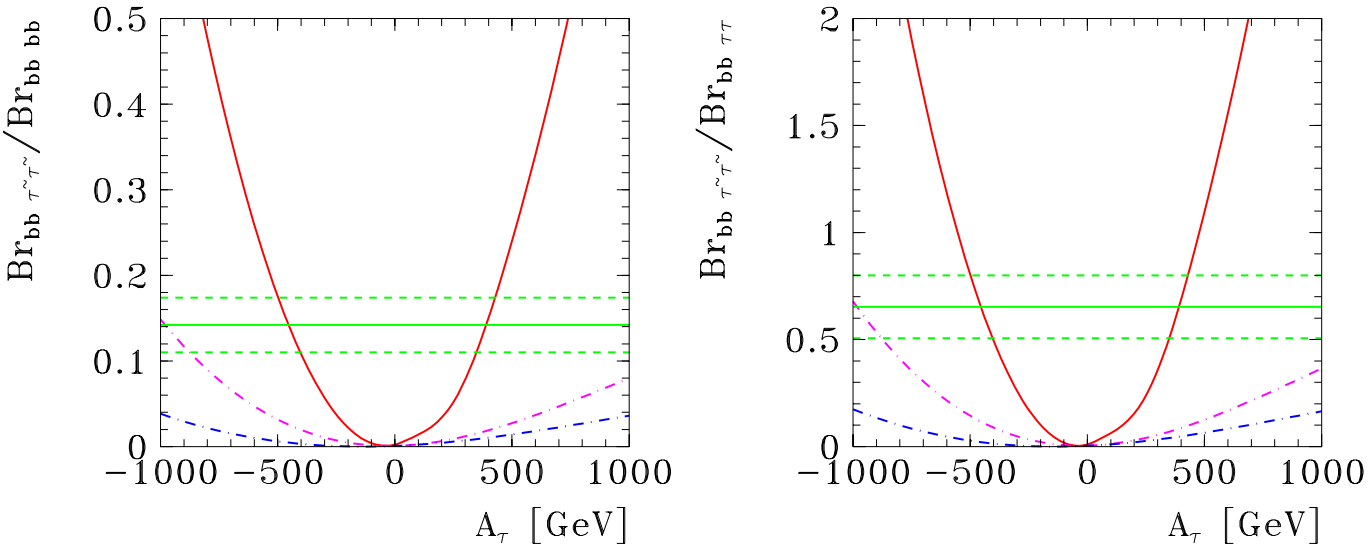

Fig. 5. Double ratios of the combined branching ratio $\mathcal{B}_{HA\to b\bar{b}\,\tilde{\tau}_i\tilde{\tau}_j}$ normalized to $\mathcal{B}_{HA\to b\bar{b}\,b\bar{b}}$ (left) and $\mathcal{B}_{HA\to b\bar{b}\,\tau\tau}$ (right) as a function of A_τ. The lower curves show the contributions from diagonal pairs $\tilde{\tau}_2\tilde{\tau}_2$ (blue) and $\tilde{\tau}_1\tilde{\tau}_1$ (magenta). The horizontal (green) lines indicate the expected experimental accuracy based on 10,000 HA decays in scenario SPS1a′

$$= \frac{\Gamma(A\to\tilde{\tau}_1\tilde{\tau}_2)}{\Gamma(A\to b\bar{b})} + \frac{\Gamma(H\to\tilde{\tau}_i\tilde{\tau}_j)}{\Gamma(H\to b\bar{b})}\,, \tag{11}$$

$$\frac{\mathcal{B}_{b\bar{b}\,\tilde{\tau}_i\tilde{\tau}_j}}{\mathcal{B}_{b\bar{b}\,\tau\tau}} = \frac{\mathcal{B}(H\to b\bar{b})\,\mathcal{B}(A\to\tilde{\tau}_1\tilde{\tau}_2) + \mathcal{B}(A\to b\bar{b})\,\mathcal{B}(H\to\tilde{\tau}_i\tilde{\tau}_j)}{\mathcal{B}(H\to b\bar{b})\,\mathcal{B}(A\to\tau\tau) + \mathcal{B}(A\to b\bar{b})\,\mathcal{B}(H\to\tau\tau)}$$

$$= \frac{\Gamma(A\to\tilde{\tau}_1\tilde{\tau}_2)}{\Gamma(A\to\tau\tau)\,(1+r)} + \frac{\Gamma(H\to\tilde{\tau}_i\tilde{\tau}_j)}{\Gamma(H\to\tau\tau)\,(1+1/r)}$$

$$= \frac{1}{2}\left[\frac{\Gamma(A\to\tilde{\tau}_1\tilde{\tau}_2)}{\Gamma(A\to\tau\tau)} + \frac{\Gamma(H\to\tilde{\tau}_i\tilde{\tau}_j)}{\Gamma(H\to\tau\tau)}\right]. \tag{12}$$

In the second double ratio the two terms in the denominator have been identified, i.e.

$$r = \frac{\Gamma(A\to b\bar{b})\;\Gamma(H\to\tau\tau)}{\Gamma(H\to b\bar{b})\;\Gamma(A\to\tau\tau)} = 1, \tag{13}$$

which is expected to hold with high accuracy.

These double ratios are proportional to $(A_\tau+\mu\cot\beta)^2 \simeq A_\tau^2$ in the decoupling limit for large A_τ and large $\tan\beta$ when LR decays dominate over the diagonal LL and RR decays and mixing can be neglected. For the parameters chosen in this study, however, we must include corrections from LR mixing of the particles and the diagonal LL and RR decays.

The pseudoscalar Higgs boson A couples to off-diagonal $\tilde{\tau}_1\tilde{\tau}_2$ pairs with the same amplitude as to $\tilde{\tau}_L\tilde{\tau}_R$ pairs so that no mixing corrections need be applied. In contrast, the coupling of the scalar Higgs boson H to off-diagonal stau pairs is modified by the mixing parameter $\cos 2\theta_{\tilde{\tau}}$ and, moreover, H decays include also contributions from the genuine diagonal couplings $\tilde{\tau}_L\tilde{\tau}_L$ and $\tilde{\tau}_R\tilde{\tau}_R$ of the order m_τ/A_τ and $m_Z/(A_\tau\tan\beta)$ with respect to the leading off-diagonal amplitudes. Since the mixing parameter

$$\sin 2\theta_{\tilde{\tau}} = \frac{2\,m_\tau}{m^2_{\tilde{\tau}_1} - m^2_{\tilde{\tau}_2}}\;(A_\tau - \mu\,\tan\beta\,) \tag{14}$$

involves A_τ itself, the dependence of the decay amplitudes on A_τ is modified and not linear anymore. As a result, the binomial character of the partial decay widths in A_τ is changed asymmetrically.

The dependence of the double ratios of the decay widths, cf. eqs. (11), (12), and (3), on A_τ including the subleading LR mixing effects are calculated using FeynHiggs [5] and are displayed in Fig. 5 together with the expected experimental accuracies. There are two possible solutions for A_τ at -450 GeV and $+350$ GeV, which, however, can be distinguished experimentally because they correspond to different $\tilde{\tau}$ mixing configurations. The mixing parameter $\sin 2\theta_{\tilde{\tau}}$ differs by $\sim$ 20 % for the two solutions. Since the mixing can be obtained with an accuracy of a few percent from measurements of the $\tilde{\tau}_1$ mass and the $\tilde{\tau}_1\tilde{\tau}_1$ production cross section at e^+e^- colliders (see [3,9] for scenarios with similar parameters), this additional information is sufficient to single out the negative A_τ solution.

From the simulation of heavy Higgs decays into supersymmetric and SM particles one obtains for the trilinear coupling

$$A_\tau = -450 \pm 50\,\text{GeV}$$

as an *ab-initio* determination of this soft SUSY breaking parameter for an event sample of 10,000 HA Higgs pairs.

Uncertainties in the theoretical predictions and parameters, eqs. (3)–(4) and their analogues for diagonal decays, are expected to be negligible at the level of achievable experimental accuracies. Theoretical calculations are under control at the per-cent level when all the one-loop corrections in the $\tilde{\tau}/\tau$ and Higgs sectors are included [10]. It is interesting to note that the parameter $\tan\beta$ can be controlled

internally within the same analysis of $HA \to b\bar{b}\,b\bar{b}$ decays. The $\tan\beta$ dependence of the combined branching ratios can be expressed as $\mathcal{B}_{b\bar{b}b\bar{b}} = 1/[(1+c_A/\tan^2\beta)(1+c_H/\tan^2\beta)]$ with coefficients $c_A \simeq 100$ and $c_H \simeq 50$ for A and H decays, respectively, in the reference point considered. From the measurement quoted in Table 3 one expects a precision of $\delta\tan\beta \simeq 0.15$. The parameter μ can be measured in chargino production within a few per-cent. Both uncertainties result in a shift of the trilinear coupling of at most $\delta A_\tau \lesssim 1\,\text{GeV}$, far below the anticipated experimental error. These estimates are confirmed by a combined analysis of SUSY parameters based on measurements of many SUSY production processes at the ILC and LHC [11].

The direct determination of the trilinear coupling analyzed in the present report may be compared with other methods which make use of higher order corrections affected by the parameter A_τ. A global analysis by means of Fittino [11] provides a combination of $X_\tau = A_\tau - \mu\tan\beta = -4450 \pm 30\,\text{GeV}$, together with $\tan\beta = 10.0 \pm 0.1$ and $\mu = 400.4 \pm 1.3\,\text{GeV}$. However, application of this indirect method is possible *a priori* only in scenarios in which the degrees of freedom are specified *in toto* when the virtual loop corrections are included and if all theoretical uncertainties are under proper control. In contrast, the proposal described in the present paper is a robust leading order analysis.

5 Summary

While the trilinear stop-Higgs coupling A_t can be measured fairly easily by evaluating the stop masses and the mixing angle, this task is much more demanding for the trilinear coupling A_τ in the stau sector since these couplings come with the masses of the quarks and leptons. Nevertheless, we have demonstrated in this report that the measurement of A_τ is possible in scalar and pseudoscalar Higgs boson H, A decays. Large luminosities at the e^+e^- linear collider ILC would be required, however, to achieve an accuracy of about 10%. Though the measurement is difficult, this direct determination based on tree-level processes is necessary before the determination through indirect effects based on quantum corrections can be trusted with high confidence.

After the stop trilinear coupling A_t will be determined, the measurement of at least one additional trilinear parameter is required to investigate universality properties of these parameters, for instance, as implemented in minimal supergravity. The A_τ measurements are therefore important ingredients for reconstructing the underlying physics scenario [12].

Acknowledgements. We are grateful to S. Heinemeyer for helpful communications on the FeynHiggs program. The work of SYC was supported in part by the Korea Research Foundation Grant (KRF-2002-041-C00081) and in part by KOSEF through CHEP at Kyungpook National University. PMZ thanks the German Science Foundation DFG and Stanford University for partial financial support during an extended visit of SLAC where part of this work was carried out.

Appendix A: Event generation

Events are generated with the program PYTHIA 6.3 [13] which includes initial and final state QED radiation as well as beamstrahlung à la CIRCE [14]. The decays of τ leptons are treated by TAUOLA [15]. The detector simulation is based on the detector proposed in the TESLA TDR [7] and implemented in the Monte Carlo program SIMDET 4.02 [16]. The main detector features are excellent particle identification and measurement of charged and neutral particles for a polar angle acceptance $\theta\ (\pi - \theta) > 125\,\text{mrad}$.

In the analysis the reconstructed b jets and τ candidates are required to be within the acceptance of $|\cos\theta| < 0.95$,

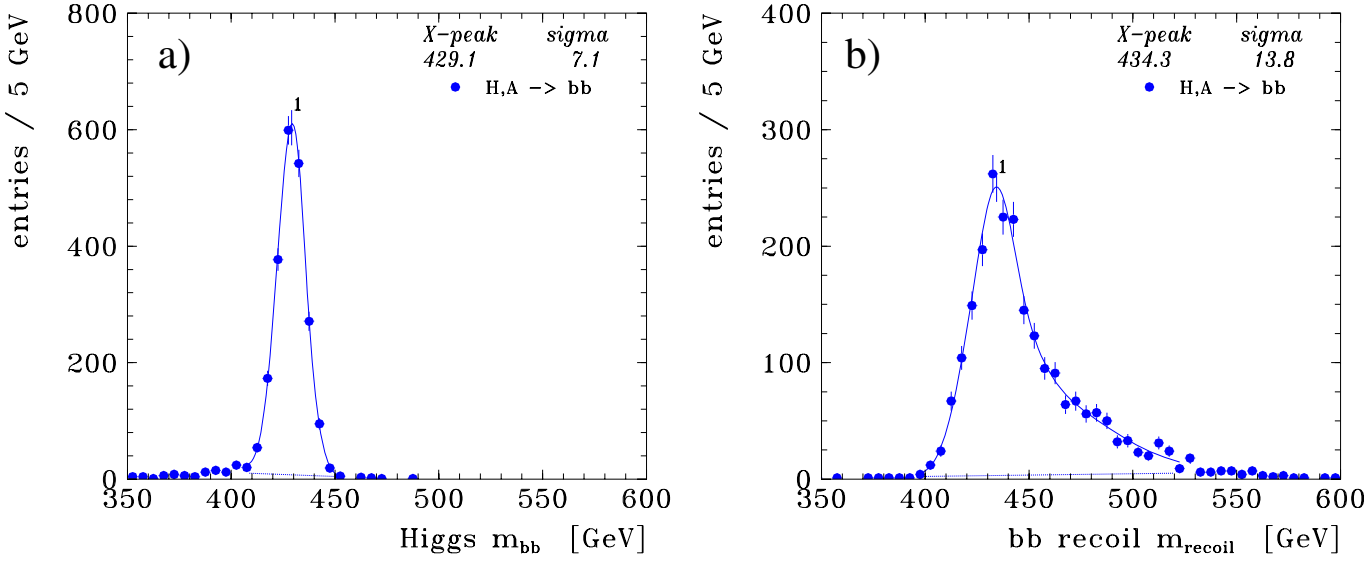

Fig. 6. Spectra from $e^+e^- \to HA \to b\bar{b}\,X$ decays of **a** bb di-jet mass m_{bb}; **b** recoil mass m_{recoil} against bb system. mSUGRA scenario SPS1a′ at $\sqrt{s} = 1\,\text{TeV}$

while Higgs boson are produced centrally $\sim \sin^2\theta$. The identification of $HA \to b\bar{b}\,X$ events is provided by the good jet energy flow measurement with a resolution of $\sigma/E = 0.3/\sqrt{E(\mathrm{GeV})}$. This is illustrated in Fig. 6, where the di-jet mass and the mass recoiling against the $b\bar{b}$ system are shown. Both distributions are fairly narrow and peak at the Higgs masses. The recoil mass spectrum is slightly wider and extends towards large values due to radiative effects.

For the identification and reconstruction of τ candidates, a narrow jet with invariant mass $m_\tau < 2.5\,\mathrm{GeV}$ is required which contains one charged particle plus possibly additional photons or three charged particles. In general the leptonic 3-body decays $\tau \to e\nu_e\nu_\tau$ (17.8%), $\tau \to \mu\nu_\mu\nu_\tau$ (17.4%) are less sensitive to the primary τ energy than the hadronic decays $\tau \to \pi\nu_\tau$ (11.1%), $\tau \to \pi^\pm\pi^0\nu_\tau$ (25.4%) and $\tau \to \pi^\pm\pi^+\pi^-\nu_\tau + \pi^\pm\pi^0\pi^0\nu_\tau$ (19.4%). All decay modes are used in the analysis, except of ee and $\mu\mu$ pairs.

Since the decay rates of interest are of the order of a few percent, to be further degraded by efficiency losses, the case study is based on a high statistics sample assuming a production rate of $N_{HA} = \sigma_{HA} \cdot \mathcal{L} = 10,000$ events. The total cross section of HA production amounts to $\sigma_{HA} = 1.8\,\mathrm{fb}$ at $\sqrt{s} = 1\,\mathrm{TeV}$, including $e^\pm$ beam polarization, QED radiation and beamstrahlung, see Fig. 1. The results of the present study may be easily transferred to any other energy or reference point once the parameters are specified.

The characteristic event signatures $HA \to b\bar{b}\,\tau\tau\,\not{E}$, i.e. two energetic b jets forming a high mass resonant state plus two τ leptons plus (possibly large) missing energy, are very clean. Any background from QCD processes $q\bar{q}(g)$, WW or ZZ production is estimated to be small and is therefore neglected.

References

1. A. Djouadi, Review The Higgs Bosons in the Minimal Supersymmetric Model, Report LPT-ORSAY-05-18, arXiv:hep-ph/0503173
2. A. Bartl, H. Eberl, S. Kraml, W. Majerotto, W. Porod, Eur. Phys. J. direct C **2**, 6 (2000)
3. E. Boos, H.-U. Martyn, G. Moortgat-Pick, M. Sachwitz, A. Sherstnev, P.M. Zerwas, Eur. Phys. J. C **30**, 395 (2003)
4. Supersymmetry Parameter Analysis: SPA Convention and Project, http://spa.desy.de/spa; B.C. Allanach et al., Eur. Phys. J. C **25**, 113 (2002)
5. S. Heinemeyer, W. Hollik, G. Weiglein, Comput. Phys. Commun. **124**, 76 (2000)
6. A. Djouadi, J. Kalinowski, P. Ohmann, P.M. Zerwas, Z. Phys. C **74**, 93 (1997)
7. TESLA Technical Design Report, DESY 2001-011, Part III: Physics at an e^+e^- Linear Collider [arXiv:hep-ph/0106315], Part IV: A Detector for TESLA
8. K. Desch, T. Klimkovich, T. Kuhl, A. Raspereza, Linear Collider note LC-PHSM-2004-006, arXiv:hep-ph/0406229
9. H.-U. Martyn, contribution to 3rd Workshop of ECFA/DESY LC Study, 2002, Prague, LC-PHSM-2003-071, arXiv:hep-ph/0406123
10. J. Guasch, W. Hollik, J. Sola, JHEP **0210**, 040 (2002); S. Heinemeyer, W. Hollik, J. Rosiek, G. Weiglein, Eur. Phys. J. C **19**, 535 (2001)
11. P. Bechtle, K. Desch, P. Wienemann, Proceedings International Linear Collider Workshop 2005, Stanford, USA, arXiv:hep-ph/0506244
12. G.A. Blair, W. Porod, P.M. Zerwas, Phys. Rev. D **63**, 017703 (2001); Eur. Phys. J. C **27**, 263 (2003)
13. T. Sjöstrand et al., Comput. Phys. Commun. **135**, 238 (2001)
14. T. Ohl, Comput. Phys. Commun. **101**, 269 (1997)
15. S. Jadach et al., Comput. Phys. Commun. **76**, 361 (1993)
16. M. Pohl, J. Schreiber, DESY 02-061, arXiv:hep-ex/0206009